



Fetal heart quantification ultrasound technology for the quantitative analysis of fetal cardiac morphology and function in hypertensive disorders of pregnancy

Yao Peng^{1#}, Wei Feng^{2#}, Chang-Xiu Yu², Cai-Hong Chang¹, Xue Liao¹, Ling Gan^{1,2}, Jia-Qi Zhang^{1,2^}

¹Department of Ultrasound Imaging, Postgraduate Union Training Base of Xiangyang No. 1 People's Hospital, School of Medicine, Wuhan University of Science and Technology, Xiangyang, China; ²Hubei Provincial Clinical Research Center for Accurate Fetus Malformation Diagnosis, Department of Ultrasound, Xiangyang No. 1 People's Hospital, Hubei University of Medicine, Xiangyang, China

Contributions: (I) Conception and design: JQ Zhang, L Gan; (II) Administrative support: JQ Zhang, L Gan; (III) Provision of study materials or patients: W Feng; (IV) Collection and assembly of data: Y Peng, W Feng; (V) Data analysis and interpretation: Y Peng, CX Yu, X Liao, CH Chang; (VI) Manuscript writing: All authors; (VII) Final approval of manuscript: All authors.

[#]These authors contributed equally to this work.

Correspondence to: Ling Gan, MS; Jiaqi Zhang, MD. Department of Ultrasound imaging, Postgraduate Union Training Base of Xiangyang No. 1 People's Hospital, School of Medicine, Wuhan University of Science and Technology, No. 15 Jiefang Road, Xiangyang 441000, China; Hubei Provincial Clinical Research Center for Accurate Fetus Malformation Diagnosis, Department of Ultrasound, Xiangyang No. 1 People's Hospital, Hubei University of Medicine, Xiangyang, China. Email: xyycs@163.com; 347235272@qq.com.

Background: Hypertensive disorders of pregnancy (HDP) are associated with adverse outcomes for both the mother and fetus, including impaired fetal cardiac development and function. Accurate assessment of fetal heart morphology and function is essential for the early detection and management of potential complications. This study investigated the clinical application value of fetal heart quantification (Fetal HQ) technology in evaluating the cardiac morphology and function in fetuses from pregnancies affected by HDP.

Methods: This prospective study examined 43 fetuses from singleton pregnancies complicated by HDP [mean gestational age (GA) 29.5±2.8 weeks] and 50 fetuses from normal pregnancies (mean GA 29.2±2.4 weeks). All participants underwent fetal ultrasonography from August 2023 to July 2024. Fetal HQ technology, incorporating two-dimensional speckle-tracking echocardiography (2D-STE) with quantitative analysis of cardiac segments, was used to assess heart size, shape, ventricular structure, contractility, and function.

Results: The HDP group exhibited significantly altered maternal clinical characteristics, including higher maternal weight, BMI, and blood pressure. Fetal cardiac morphometry indicated that compared to the control group, the HDP group had larger left ventricular (LV) dimensions yet lower volumes but had smaller right ventricular (RV) dimensions. Notably, compared with the control group, the HDP group had a larger LV end-diastolic (ED) area (2.52±0.88 vs. 1.92±0.62 cm²; P<0.001) and ED length (2.35±0.37 vs. 1.89±0.33 cm; P<0.001) but a smaller LV ED volume (2.17±0.83 vs. 3.09±0.69 mL; P<0.001). Additionally, the HDP group exhibited significantly higher LV global strain (−30.53%±9.88% vs. −25.22%±8.33%; P=0.006), indicating altered cardiac function. The 24-segment analysis revealed notable alterations in ventricular geometry and function within the HDP group, with lower sphericity index (SI) and fractional shortening (FS) values across various segments of both ventricles. These findings closely align with the results of the Z score analysis, further highlighting the extent of cardiac dysfunction.

[^] ORCID: Yao Peng, 0009-0004-1305-4558; Jia-Qi Zhang, 0000-0003-2234-1730.

Conclusions: Fetal HQ technology effectively identified significant alterations in fetal heart structure and function in pregnancies complicated by HDP. These findings suggest that Fetal HQ is a useful tool for the early detection of fetal heart abnormalities and can facilitate timely intervention and accurate prognosis in affected pregnancies.

Keywords: Hypertensive disorders of pregnancy (HDP); fetal cardiac morphology; fetal cardiac function; fetal heart quantification technology (Fetal HQ technology); ultrasound imaging

Submitted Jul 30, 2024. Accepted for publication Feb 11, 2025. Published online Mar 28, 2025.

doi: 10.21037/qims-24-1553

View this article at: <https://dx.doi.org/10.21037/qims-24-1553>

Introduction

Hypertensive disorders of pregnancy (HDP) are conditions characterized by elevated blood pressure that occur during pregnancy and affect approximately 5–10% of pregnancies. These disorders significantly impact maternal, fetal, and neonatal outcomes (1). HDP primarily presents as hypertension and proteinuria, which can lead to systemic dysfunction or failure of multiple organs during pregnancy. In critical conditions, HDP may result in convulsions, coma, or even death. Notably, HDP accounts for approximately 10% to 16% of all pregnancy-related maternal deaths and thus is the second-leading direct cause of maternal mortality (2).

There is currently no unified international standard for the classification of HDP (3). Based on the International Society for the Study of Hypertension in Pregnancy (ISSHP), HDP is categorized into two main types: the first type includes hypertension diagnosed before pregnancy or discovered before 20 weeks of gestation, while the second type includes hypertension occurring after 20 weeks of gestation (≥ 20 weeks) (4). Hypertension in pregnancy causes constriction and spasms of the small arteries throughout the pregnant woman's body, thereby increasing blood flow resistance and damaging the maternal heart. Moreover, it leads to constriction and spasms of the small arteries on the maternal side of the placenta, which reduces the placenta's blood and oxygen exchange function. As a result, fetal growth and development can be impaired, elevating the risk of placental abruption, fetal ischemia and hypoxia, preterm birth, and even death. The fetal heart's endocardium is particularly sensitive to ischemia and hypoxia. Consequently, accurately assessing fetal heart function changes in the context of HDP can provide early indicators of fetal hypoxia in utero. This is crucial for evaluating fetal changes under HDP and may aid clinicians in understanding fetal oxygenation and development, predicting perinatal

outcomes, and enacting timely intervention and accurate prognosis (5).

Ultrasonography has been widely applied in the evaluation of ventricular function (6). The development and application of traditional two-dimensional ultrasound, M-mode ultrasound, and Doppler ultrasound technologies have facilitated this assessment of ventricular dysfunction (7). These methods typically measure atrial and ventricular diameters, left and right ventricular (RV) outflow tract diameters, relevant blood flow velocity indicators, and the myocardial performance index in characterizing ventricular diastolic and systolic function (8). However, the clinical application of traditional ultrasound indicators is limited. Accurate imaging evaluation of fetal cardiac structure and function requires precise positioning of the apex and highly specific angles for hemodynamic measurements. Furthermore, these methods primarily capture longitudinal systolic function, often overlooking overall and transverse function. Due to the uniqueness of the fetal circulatory system and the involvement of complex muscle fiber movements and ventricular rotation, traditional techniques may not fully capture changes in fetal ventricular function (9).

Fetal heart quantification (Fetal HQ) is an innovative method that combines two-dimensional speckle-tracking echocardiography (2D-STE) with quantitative analysis of cardiac segments applied to the fetal heart. Compared to traditional 2D-STE, Fetal HQ offers several advantages (10,11). First, Fetal HQ allows for automated border detection of the endocardium, which reduces operator dependency and variability, thereby enhancing measurement consistency and accuracy. Second, it provides a comprehensive assessment by evaluating longitudinal, circumferential, and radial motion, as well as overall ventricular rotation. This multidimensional analysis, which surpasses the primarily longitudinal focus of traditional 2D

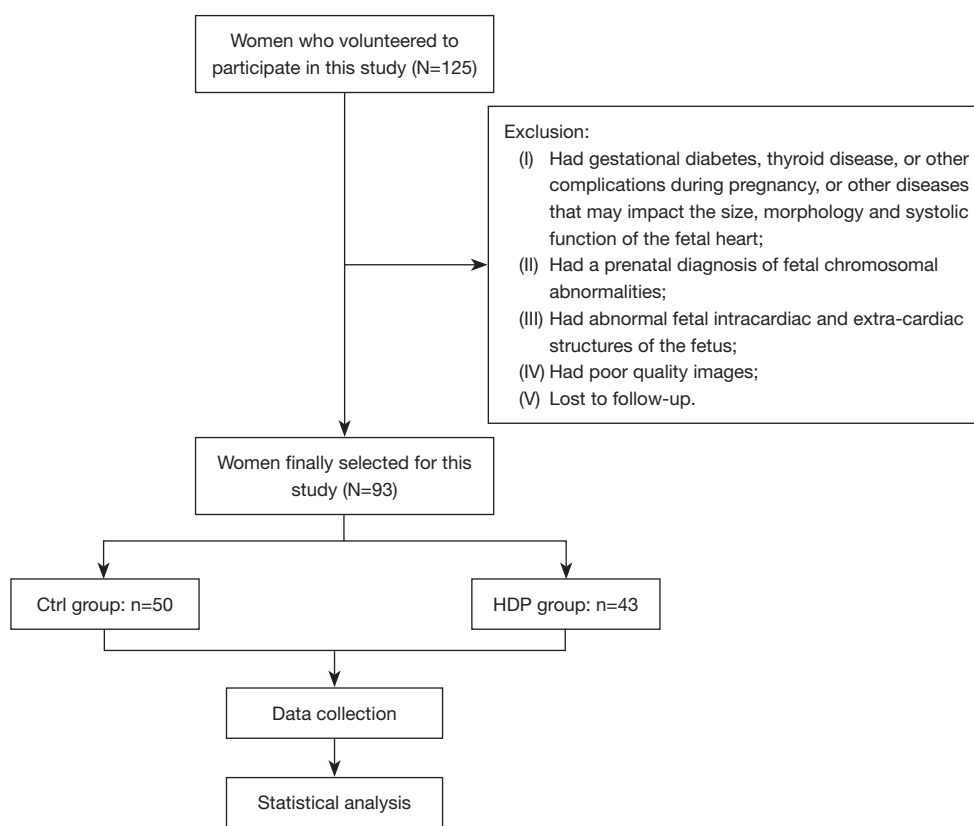


Figure 1 Study recruitment flowchart. Ctrl, control; HDP, hypertensive disorders of pregnancy.

STE, enables a more precise assessment of the structure and function of the fetal heart (12).

This study examined the value of Fetal HQ technology in assessing the morphology of the fetal heart in cases of HDP. We present this article in accordance with the STROBE reporting checklist (available at <https://qims.amegroups.com/article/view/10.21037/qims-24-1553/rc>).

Methods

Study population

A total of 125 second- and third-trimester pregnancies examined from August 2023 to July 2024 using ultrasound technology at Xiangyang No. 1 People's Hospital, affiliated with the School of Medicine, Wuhan University of Science and Technology, were initially included for analysis. After rigorous exclusion criteria were applied, 93 pregnant women and their fetuses were consecutively enrolled. Finally, 43 singleton pregnancies with hypertensive HDP with a gestational age (GA) of 29.5 ± 2.8 weeks (the HDP group)

and 50 healthy pregnancies with a GA of 29.2 ± 2.4 weeks (the control group) were included in this prospective study. The diagnosis of HDP was conducted according to the criteria outlined by the ISSHP, which considers HDP to include pregnancies in which there is high blood pressure, defined as a systolic pressure of 140 mmHg or greater and/or a diastolic pressure of 90 mmHg or greater. The inclusion criteria for patients were as follows: (I) pregnant women aged 18 years or older; (II) gestation between 25 and 35 weeks; (III) a menstrual cycle with regular intervals; and (IV) pregnancy with a single fetus. Patients who met any of the following criteria were excluded: (I) diabetes during gestation, thyroid disorders, or other concomitant conditions impacting fetal heart size, morphology, or systolic function; (II) fetal chromosomal abnormalities during the prenatal period; (III) fetal intracardiac or extracardiac structural abnormalities; (IV) poor-quality imaging; and/or (V) lost to follow-up (Figure 1).

Each participant consented to fetal ultrasonography having been fully informed of both its reliability and limitations. The study was conducted in accordance with

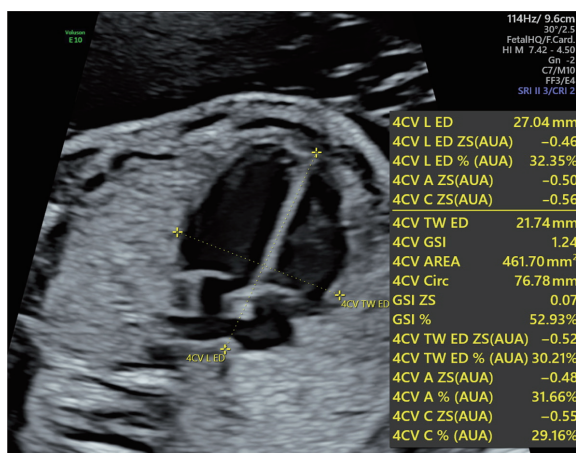


Figure 2 Computation of GSI. For the measurement of the fetal cardiac GSI of mothers with HDP, a longitudinal line is drawn from the apex to the base of the cardiac outer edge, and a transverse line is drawn from the sidewall of the LV to the sidewall of the RV at the end of diastole. The GSI can be obtained by dividing the end-diastolic basal-apical length by the end-diastolic transverse width. A, area; C, circumference; ED, end-diastolic; GSI, global sphericity index; HDP, hypertensive disorders of pregnancy; LV, left ventricle; RV, right ventricle; 4CV, four-chamber view; L, left; ZS, Z score; TW, transverse width.

the Declaration of Helsinki (as revised in 2013) and was approved by the Ethics Committee of the Xiangyang No. 1 People's Hospital, affiliated with the School of Medicine at Wuhan University of Science and Technology (approval No. 2021KYLX02). All patients in this study provided informed consent.

Assessment of maternal and fetal parameters

In clinical visits, we measured maternal age (years), height (cm), weight (kg), and body mass index (BMI). Additionally, we collected data on systolic blood pressure during the scan (mmHg), diastolic blood pressure during the scan (mmHg), triglycerides (mmol/L), total cholesterol (mmol/L), high-density lipoprotein (HDL) cholesterol (mmol/L), low-density lipoprotein (LDL) cholesterol (mmol/L), early pregnancy fasting glucose (mmol/L), GA at the time of the scan (weeks), estimated fetal weight (kg), umbilical artery pulsatility index (PI), cerebroplacental ratio, and PI of the middle cerebral artery. All pregnant women were followed up after delivery, and GA at delivery (weeks) and birth weight (kg) were recorded.

Evaluation of overall size and shape of the heart in the four-chamber view (4CV)

The Voluson E10 ultrasound system (GE HealthCare, Chicago, IL, USA) was used in conjunction with Fetal HQ for comprehensive fetal cardiac assessment. This included TomTec analysis software (TomTec Imaging Systems, Munich, Germany), the normative reference charts from Professor Devore's, Z scores, and centile assessments (10). Pregnant women were instructed to assume a supine or lateral position for a standard fetal two-dimensional ultrasound examination. The measurements of the fetal femur length and biparietal diameter were obtained to determine the GA. A routine fetal echocardiography with an apical 4CV was then performed. The heart's apex was directed toward the transducer to obtain a clear static image of the heart at the end-diastolic (ED) phase. The global sphericity index (GSI) was calculated as the quotient of the heart's longitudinal diameter divided by its transverse diameter (Figure 2).

Appraisal of ventricular shape and contractility

After completing the morphological analysis of the 4CV, we proceeded to assess ventricular contractility. First, the sampling line was positioned at the tricuspid valve, and an anatomical M-mode line was drawn from the apical segment to the basal segment. A single cardiac cycle was selected in which both diastolic and systolic phases exhibited clear endocardial motion, with complete visualization of the endocardium and uniform ventricle size. The end-systolic (ES) and ED phases were determined based on the opening and closing of the mitral and tricuspid valves. ED was defined as the frame where the atrioventricular valves were fully closed (the lowest point on the M-mode trace), while ES was defined as the frame immediately before the atrioventricular valves opened (the peak on the M-mode trace) (Figure 3).

At the end of ventricular systole, three markers were placed sequentially at the following locations: the insertion points of the interventricular septum and tricuspid valve in each of the right and left ventricles, the free wall and tricuspid valve insertion points, and the endocardium at the apex. This method allowed for the automatic identification of the margins of the endocardium within the left and right ventricles during both ED and ES, with each ventricle being divided into 24 equidistant segments. Once the endocardium was traced, the software tracked it throughout

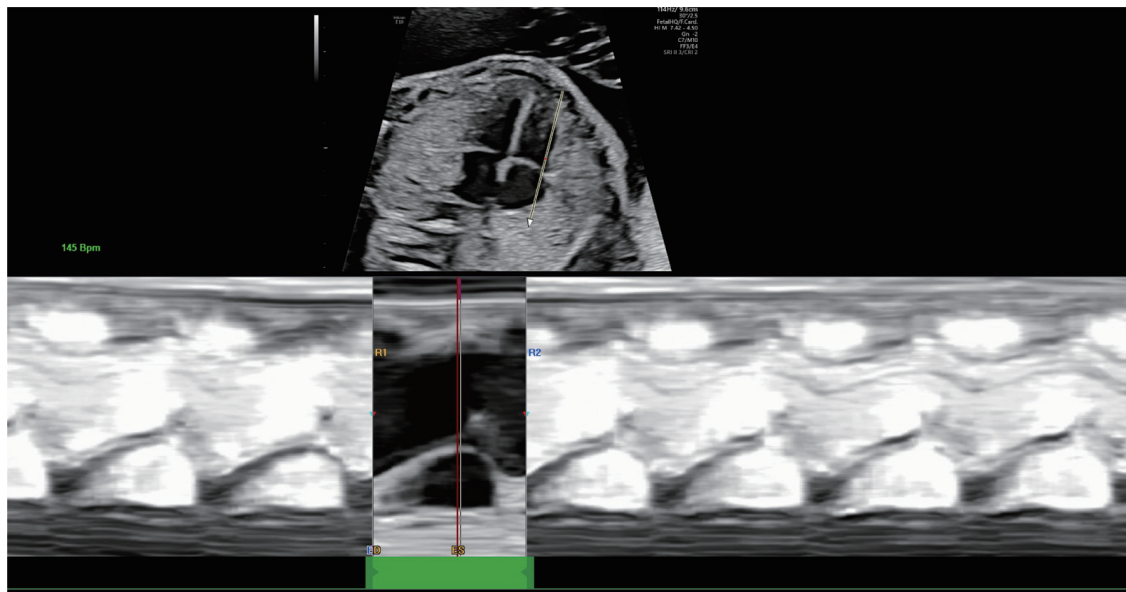


Figure 3 Determination of the cardiac cycle. This figure shows the determination of the right ventricular cardiac cycle, including end-diastolic and end-systolic.

the cardiac cycle and displayed the contours. The examiner YP and WF reviewed the cardiac cycle to ensure accurate endocardial tracking. If required, the markers were adjusted, and automatic tracking could be reapplied. The system then generated dynamic tracking curves, involving the endocardial lengths from the insertion points of the septal and atrioventricular valves to the apex, as well as from the apex to the insertion points of the atrioventricular valves on the lateral wall. For each ventricle, segments 1–8 were designated as the basal segments, segments 9–16 as the midsegments, and segments 17–24 as the apical segments. We generated a detailed analysis report of the overall cardiac function and evaluations of all 24 segments. From this, data regarding the ED diameters of the left and right ventricles, along with global longitudinal strain (GLS), fractional area change (FAC), 24-segment sphericity index (SI), and fractional shortening (FS) were gathered. The Z score method was applied to comprehensively assess the entire heart of the fetus and its functional parameters. In addition, the recorded cardiac parameters included left ventricular ED (LVED) area, LVED volume (LVEDV), LVES area, LVES volume (LVESV), LVED length, LVES length, right ventricular ED (RVED) area, RVED length, RVES area, RVES length, 4CV width at ED, 4CV length at ED, 4CV circumference, and 4CV area (*Figure 4*).

The echocardiographer was informed of the study

objectives but remained unaware of the classification and ultrasonic diagnostic results. To assess the intra- and interobserver variability, the original echocardiographer (Y.P.) and the second examiner (W.F.) performed speckle-tracking analysis once more on 15 randomly chosen cases after an interval of 1 month. Statistical analysis and Bland-Altman plots were used to evaluate the degree of variation. Intraclass correlation coefficient (ICC) values above 0.75 indicated good reliability, while values exceeding 0.9 indicated excellent reliability.

Statistical analysis

The Kolmogorov-Smirnov test was first employed to check the normality of quantitative variables. Variables with a normal distribution are expressed as the mean \pm standard deviation. For data that did not follow a normal distribution, the Kruskal-Wallis test was applied to determine differences between the groups. In the case of a significant difference, pairwise comparisons were carried out. For variables with a normal distribution, paired *t* tests with Bonferroni corrections were implemented. The Spearman correlation coefficient was employed to evaluate the relationships among maternal traits, metabolic parameters, and fetal cardiac indices. Statistical significance was defined as a P value less than 0.05. SPSS version 26.0

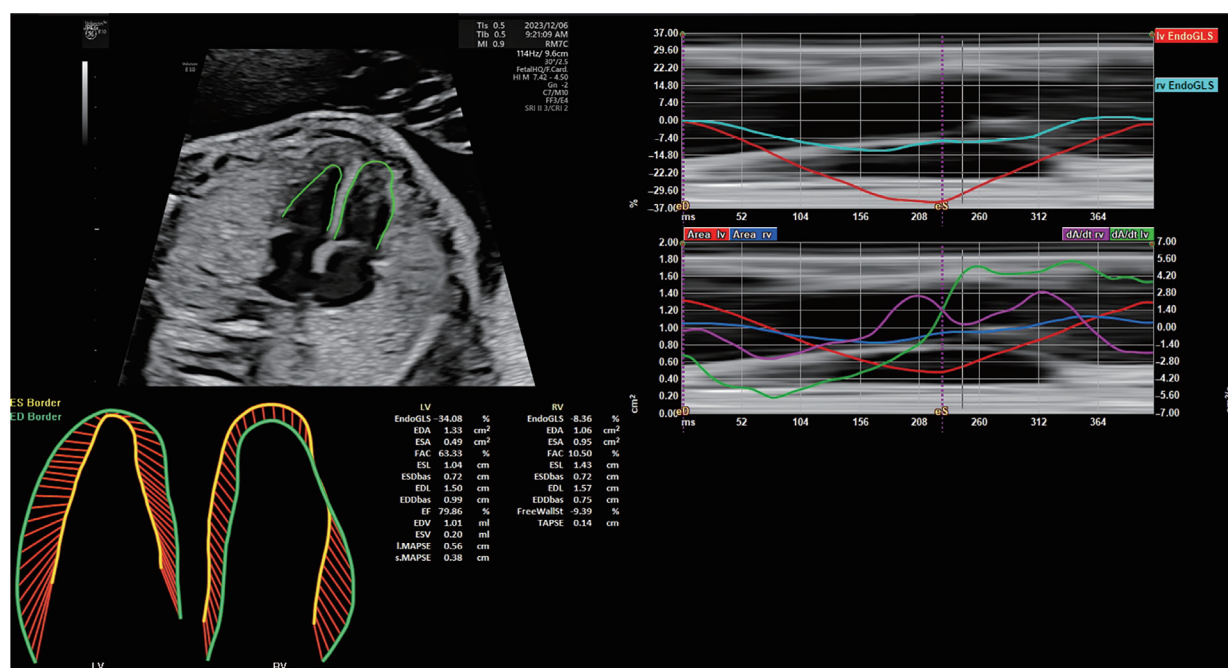


Figure 4 A 24-segment speckle-tracking measurement by Fetal HQ analysis. The green lines delineate the endocardial borders of the ventricular walls, illustrating their morphology and dimensions for analysis. Fetal HQ, fetal heart quantification.

(IBM Corp., Armonk, NY, USA) was used to conduct all statistical analyses.

Results

Participant characteristics

Initially, 125 pregnant women underwent prenatal ultrasound examinations. Among them, 12 women had gestational diabetes, thyroid disease, or other complications that could potentially influence the systolic function, morphology, or size of the fetal heart. Additionally, seven women were diagnosed prenatally with abnormalities of fetal chromosomes, eight had abnormal structures either within the heart or outside the heart, and six had poor-quality images. Furthermore, five participants did not complete follow-up. Consequently, the final study cohort included 50 women without HDP and 43 women with HDP (Figure 1).

The HDP group and the control group showed marked differences in general clinic characteristics. The HDP group had a higher maternal weight, estimated fetal weight, birth weight, BMI, and blood pressure; a more adverse lipid profile; and an earlier delivery time. Specifically, the HDP group had elevated levels of triglycerides, total cholesterol, and LDL cholesterol, while the HDL cholesterol level was

similar between the groups. We detected no significant disparities in the umbilical artery PI, cerebroplacental ratio, or middle cerebral artery PI (Table 1).

Fetal heart structure

Fetal HQ was conducted to compare the alterations in fetal cardiac morphometry between the HDP group and the control group. Fetal cardiac morphometry indicated that the HDP group had larger LV dimensions yet reduced volumes but smaller right ventricular dimensions as compared to the control group. More specifically, the HDP group had a significantly larger LVED area and LVED length and a larger LVES area ($P < 0.001$). Conversely, the HDP group had significantly smaller LVEDV but larger ES volume. Regarding the RV, the HDP group exhibited significantly smaller ED area and ED length. No significant differences were observed in the RVES area or in the parameters of the 4CV, including GSI, length, width, circumference, and area (Table 2).

Fetal heart function

Fetal HQ was conducted to compare fetal heart function between the HDP and control groups. The LV global strain

Table 1 Demographic characteristics and pregnancy outcomes

Variable	HDP (N=43)	Control (N=50)	P value	Clinical reference range
Maternal age (years)	31.3±4.8	30.8±4.2	0.593	–
Height (cm)	160.4±6.8	161.8±5.6	0.279	–
Weight (kg)	70.1±5.5	61.6±4.7	<0.001	–
BMI (kg/m ²)	27.8±6.1	24.5±5.3	<0.01	<25 (normal)
SBP at scan (mmHg)	155.2±7.7	108.6±6.5	<0.001	≥140 (hypertension)
DBP at scan (mmHg)	102.5±6.8	74.9±5.5	<0.001	≥90 (hypertension)
Triglycerides (mmol/L)	3.55±1.35	2.56±0.73	<0.001	<1.7 (optimal)
Total cholesterol (mmol/L)	6.84±1.36	5.89±1.04	<0.001	<5.2 (desirable)
HDL cholesterol (mmol/L)	1.56±0.65	1.57±0.42	0.929	> 1.0 (optimal)
LDL cholesterol (mmol/L)	3.24±0.85	2.18±0.54	<0.001	<2.6 (optimal)
Early pregnancy fast glucose (mmol/L)	4.95±0.70	4.86±0.52	0.480	<5.1 (normal)
GA at delivery (weeks)	39.29±0.54	40.21±0.41	<0.001	37–42 (term delivery)
GA at scan (weeks)	29.5±2.8	29.2±2.4	0.579	–
Estimated fetal weight (kg)	1.09±0.23	1.01±0.17	0.058	–
Birth weight (kg)	3.52±0.48	3.24±0.56	<0.05	≥2.5 (normal)
Umbilical artery PI	1.18±0.13	1.15±0.09	0.194	<1.20 (normal)
Middle cerebral artery PI	2.15±0.31	2.09±0.27	0.321	1.3–2.5 (depending on GA)
Cerebroplacental ratio	1.97±0.32	1.94±0.27	0.625	>1.0 (normal)

Data are given as the mean ± standard deviation. Clinical reference ranges are based on established guidelines. BMI, body mass index; DBP, diastolic blood pressure; GA, gestational age; HDP, hypertensive disorders of pregnancy; HDL, high-density lipoprotein; LDL, low-density lipoprotein; PI, pulsatility index; SBP, systolic blood pressure.

in the HDP group was significantly higher than that of the control group ($-30.53\% \pm 9.88\%$ *vs.* $-25.22\% \pm 8.33\%$; $P=0.006$), suggesting an alteration in cardiac function. However, no notable differences were detected in RV global strain, LV FAC, RV FAC, LV ejection fraction, LV stroke volume, or LV cardiac output between the HDP and control groups (*Table 3*).

Twenty-four-segment analysis

Comparison of segmental ventricular ED values

The fetal heart rate differed significantly between the HDP group and the control group. Segments 12–24 of the LV in the HDP group had significantly greater ED values than did those in the control group, with segment 15 (12.01 ± 2.48 *vs.* 10.17 ± 2.85 mm; $P=0.001$) and segment 20 (9.97 ± 2.36 *vs.* 8.06 ± 2.41 mm; $P<0.001$) being particularly high. Similarly, segments 12–19 and segment 24 of the RV

in the HDP group had significantly greater ED values than did those in the control group, with segment 16 (10.13 ± 2.24 *vs.* 9.10 ± 1.80 mm; $P=0.016$) and segment 19 (7.87 ± 1.92 *vs.* 7.23 ± 0.81 mm; $P=0.035$) being particularly high. The results suggest that fetuses in the HDP group had altered ventricular morphometry, with numerous segments in both the LV and RV exhibiting considerably larger ED values (*Figure 5*).

Differences in the SI values of segmental ventricles

SI analysis revealed significant differences in ventricular geometry between the HDP group and control group, particularly in the later stages. This finding emphasizes the impact of hypertensive disorders during pregnancy upon the structure of the fetal heart. Significant disparities in the 24-segment SI values of the ventricles were identified between the two groups. In segments 8–24, the HDP group had significantly reduced SI values for the LV, reflecting an

Table 2 Comparison of fetal cardiac morphometry findings of the patients

Variable	HDP (N=43)	Control (N=50)	P value	Clinical reference range
LVED area (cm ²)	2.52±0.88	1.92±0.62	<0.001	1.8–2.5
LVED length (cm)	2.35±0.37	1.89±0.33	<0.001	1.8–2.4
LVES area (cm ²)	1.72±0.52	1.29±0.48	<0.001	1.1–1.6
LVES length (cm)	1.83±0.46	1.75±0.32	0.328	1.5–2.0
LVEDV (mL)	2.17±0.83	3.09±0.69	<0.001	2.0–3.5
LVESV (mL)	1.47±0.58	1.05±0.52	<0.001	0.9–1.5
RVED area (cm ²)	1.47±0.29	1.79±0.35	<0.001	1.5–2.0
RVED length (cm)	1.38±0.35	1.74±0.39	<0.001	1.6–2.0
RVES area (cm ²)	1.16±0.53	1.34±0.58	0.124	1.0–1.4
RVES length (cm)	1.18 ± 0.24	1.58±0.20	<0.001	1.4–1.8
4CV GSI	1.16 ± 0.18	1.19 ± 0.11	0.328	1.1–1.3
4CV width ED (mm)	33.63±5.91	33.90±5.42	0.819	32–36
4CV length ED (mm)	39.42±7.53	39.14±5.50	0.837	37–41
4CV area (mm ²)	1011.45±129.87	1011.36±140.65	0.997	950–1100
4CV circ (mm)	115.38±18.93	113.24±19.49	0.594	110–120

Data are given as the mean ± standard deviation. Clinical reference ranges are based on standard fetal echocardiography guidelines. circ, circumference; ED, end-diastolic; ES, end-systolic; GSI, global spherical index; LV, left ventricle; RV, right ventricle; V, volume; 4CV, four-chamber view.

Table 3 Comparison of fetal cardiac function findings of the patients

Variable	HDP (N=43)	Control (N=50)	P value	Clinical reference range
LV global strain (%)	−30.53±9.88	−25.22±8.33	<0.01	−16 to −30
RV global strain (%)	−18.45±8.18	−16.93±9.92	0.427	−16 to −24
LV FAC (%)	47.49±15.96	50.38±14.11	0.357	≥45
RV FAC (%)	34.73±14.90	38.78±13.54	0.173	≥35
LV EF (%)	51.63±13.47	52.85±12.34	0.649	≥50
LV SV (mL)	1.12±0.82	0.96±0.95	0.391	0.8–1.5
LV CO (mL/min)	153.62±73.56	128.38±84.72	0.132	120–180

Data are given as the mean ± standard deviation. Clinical reference ranges are based on standard fetal echocardiography guidelines. CO, cardiac output; EF, ejection fraction; FAC, fractional area change; HDP, hypertensive disorders of pregnancy; LV, left ventricle; RV, right ventricle; SV, stroke volume.

altered geometry. Key differences between the HDP group and control group in the LV were observed for segment 8 (1.58±0.33 *vs.* 1.84±0.43; *P*=0.002), segment 10 (1.60±0.42 *vs.* 1.89±0.48; *P*=0.003), segment 12 (1.66±0.34 *vs.* 2.03±0.37; *P*<0.001), segment 16 (1.81±0.45 *vs.* 2.27±0.45; *P*<0.001), segment 18 (1.90±0.50 *vs.* 2.43±0.43; *P*<0.001), and segment 20 (2.13±0.80 *vs.* 2.78±0.58; *P*<0.001); for the

RV, significant differences were observed in segment 16 (1.72±0.41 *vs.* 1.98±0.43; *P*=0.004), segment 17 (1.85±0.42 *vs.* 2.63±0.40; *P*<0.001), segment 18 (2.03±0.44 *vs.* 2.72±0.42; *P*<0.001), 19 (2.26±0.48 *vs.* 2.73±0.38; *P*<0.001), segment 20 (2.59±0.52 *vs.* 2.83±0.52; *P*<0.001), segment 21 (2.82±0.74 *vs.* 3.42±0.84; *P*=0.001), and segment 24 (12.63±1.75 *vs.* 11.22±2.73; *P*=0.004) (*Figure 6*).

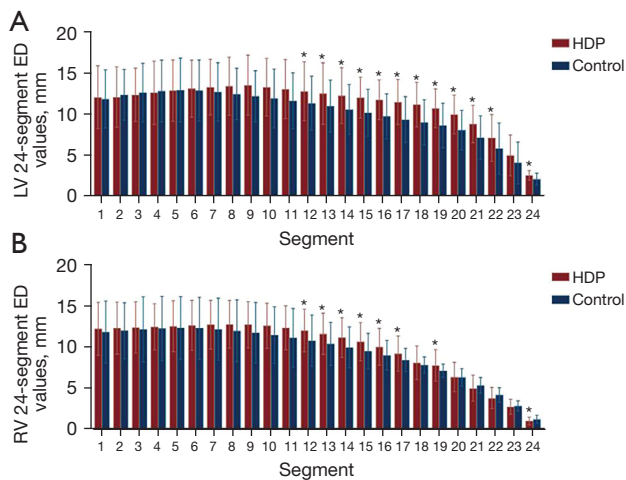


Figure 5 Comparison of ventricular 24-segment ED values between groups. *, P value <0.05. ED, end-diastolic; HDP, hypertensive disorders of pregnancy; LV, left ventricle; RV, right ventricle.

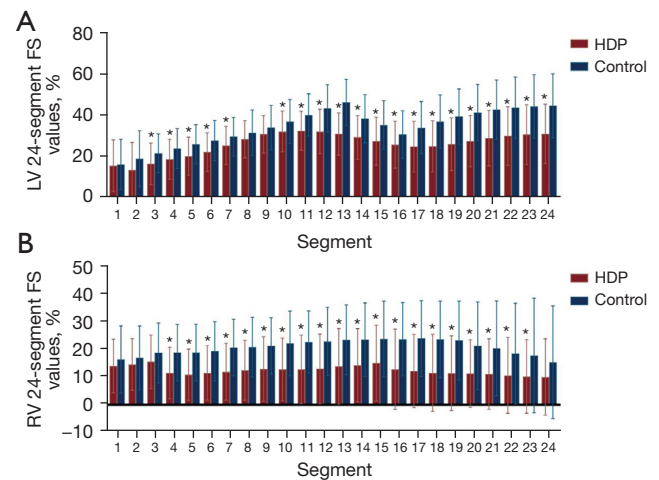


Figure 7 Comparison of ventricular 24-segment FS values between groups. *, P value <0.05. FS, fractional shortening; HDP, hypertensive disorders of pregnancy; LV, left ventricle; RV, right ventricle.

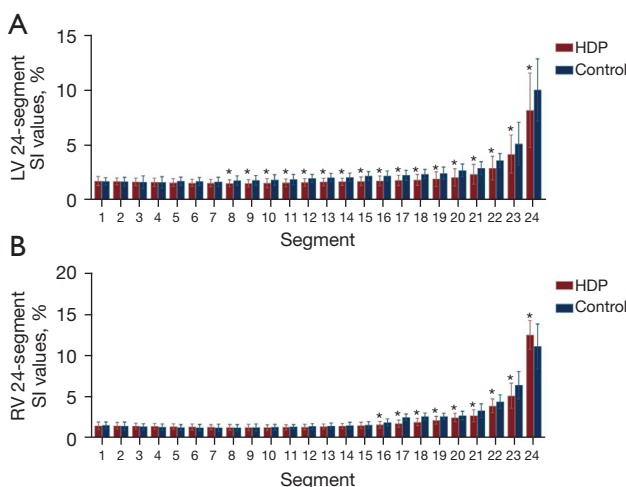


Figure 6 Comparison of ventricular 24-segment SI values between groups. *, P value <0.05. HDP, hypertensive disorders of pregnancy; LV, left ventricle; RV, right ventricle; SI, sphericity index.

Differences in the FS values of the segmental ventricles

The HDP group demonstrated significantly lower FS values in multiple segments for both the LV and RV, indicating impaired ventricular function in fetuses affected by HDP. When the 24-segment FS values of the HDP group and the control group were compared, marked differences were evident. Specifically, the LV of the HDP group had lower

FS values in segments 3 to 24, with significant differences in segment 12 ($32.07\% \pm 10.73\%$ vs. $43.31\% \pm 11.38\%$; $P < 0.001$) and segment 19 ($25.96\% \pm 12.74\%$ vs. $39.34\% \pm 13.32\%$; $P < 0.001$). Similarly, the RV in the HDP group exhibited markedly lower FS values in segments 4–23. Specifically, there were significant differences in segment 4 ($11.47\% \pm 9.35\%$ vs. $18.88\% \pm 10.23\%$; $P < 0.001$) and segment 19 ($11.42\% \pm 13.56\%$ vs. $23.27\% \pm 14.29\%$, $P < 0.001$) (Figure 7).

Comparison of FS Z score values of the segmental ventricles

The HDP group showed significantly lower FS Z score across multiple segments in both the LV and RV as compared with the control group, indicating impaired global ventricular function. Specifically, for the LV, the HDP group exhibited a markedly lower FS Z score in segments 3–24, with significant differences in segment 12 (-1.92 ± 0.95 vs. -0.46 ± 0.82 ; $P = 0.043$) and segment 16 (-1.83 ± 0.67 vs. -0.65 ± 0.83 ; $P < 0.001$). Similarly, the RV in the HDP group demonstrated markedly lower FS Z score values in segments 2–22, with significant differences in segment 12 (-2.17 ± 0.90 vs. -1.04 ± 0.80 ; $P = 0.043$) and segment 19 (-1.86 ± 0.72 vs. -1.12 ± 0.70 ; $P = 0.035$) (Figure 8).

Intra- and interobserver reliability for Fetal HQ heart measurements

In this study, we applied the ICC to assess the intra- and interobserver reliability of different cardiac measurements to

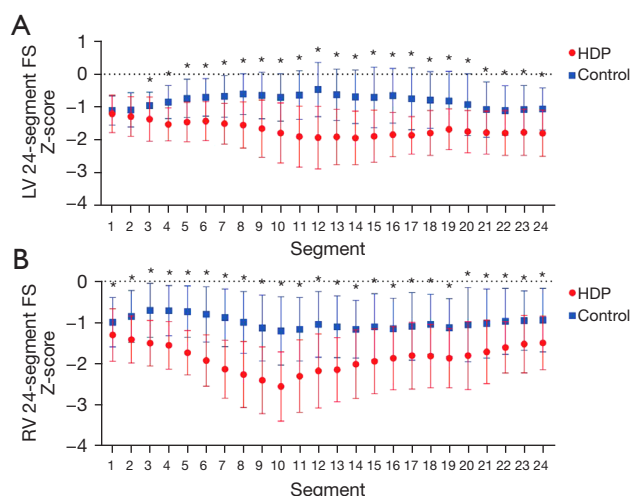


Figure 8 Comparison of ventricular 24-segment FS Z score values between groups. *, P value < 0.05. FS, fractional shortening; HDP, hypertensive disorders of pregnancy; LV, left ventricle; RV, right ventricle.

ensure the consistency and accuracy of these measurements. It was found that the LV GLS had a positive correlation with maternal age but a negative correlation with maternal weight and BMI. Moreover, the fasting glucose levels of pregnant women the early pregnancy exhibited a negative correlation with 4CV area, 4CV ED, 4CV length ED, 4CV GSI, 4CV GSI%, RVES length, RVES area, RVES length, RVES area, LV cardiac output, and LV stroke volume. Glycated hemoglobin (HbA1c) levels were negatively correlated with 4CV area, 4CV width ED, and 4CV length ED. Finally, total cholesterol and LDL cholesterol were negatively correlated with RV FAC and RV GLS (*Table 4*).

Discussion

HDP represent a significant obstetric complication that are unique to pregnancy, posing substantial risks to both maternal and fetal health (13). This condition is closely linked with unfavorable birth outcomes, such as premature delivery, low birth weight, and perinatal mortality. As the maternal age and obesity rates has increased, the incidence of pregnancy-related complications, particularly gestational hypertension, has similarly risen (14). Various risk factors contribute to the onset of gestational hypertension, including maternal obesity, dietary habits, and genetic predispositions (15). Elevated maternal blood pressure may trigger the narrowing of placental blood vessels and

an increase in vascular resistance, leading to placental dysfunction. This dysfunction impairs the uterine-placental blood supply, prevents the fetus from receiving adequate nutrition, and induces inflammatory responses in both the mother and fetus (16). In addition, compensatory mechanisms may cause insufficient peripheral blood flow and ischemia, adversely affecting fetal growth and development (17). Given the high sensitivity of the fetal endocardium to hypoxia, it is imperative to quantitatively evaluate fetal cardiac function in the context of HDP, as these assessments can provide critical insights for early intervention and clinical management.

Recent advancements in ultrasonography, including two-dimensional, M-mode, and Doppler imaging, have improved the evaluation of ventricular function (18). However, these traditional methods often encounter difficulties in providing precise measurements and are predominantly focused on longitudinal systolic function, with broader and transverse aspects of ventricular performance being ignored. Moreover, these techniques may not fully capture fetal ventricular function due to the complex nature of fetal circulation and ventricular movements (19).

Fetal HQ technology is a novel approach that integrates 2D STE with other advanced techniques for fetal cardiac assessment (20). This method allows for independent tracking of the endocardial boundaries related to the left and right ventricles of the fetus, which are divided into 24 uniformly spaced parts for the quantitative analysis of contractility and size. Fetal HQ technology combines 2D-STE with cardiac segmental quantification, addressing several limitations of traditional 2D-STE in the evaluation fetal cardiac structure and function. Compared to conventional 2D-STE, Fetal HQ technology offers distinct advantages (21). First, it minimizes operator dependence through automatic boundary detection, whereas traditional 2D-STE relies on manual boundary delineation, which is significantly influenced by the operator's skill and experience (22). Automated detection in Fetal HQ technology reduces human error and enhances measurement consistency and reliability, also decreasing the time required for repeated measurements. Second, Fetal HQ technology enables multidimensional cardiac motion assessment (23). While traditional 2D-STE primarily focuses on longitudinal contractile function, Fetal HQ provides a comprehensive evaluation of longitudinal, circumferential, and radial motion, as well as overall ventricular rotation (24). This extensive approach facilitates a more detailed and accurate assessment of the fetal heart's functional state from multiple

Table 4 Intrarater and interrater reliability for Fetal HQ cardiac measurements

Cardiac parameter	Intrarater		Interrater	
	ICC	95% confidence interval	ICC	95% confidence interval
LV GLS	0.749	0.528–0.935	0.628	0.417–0.833
RV GLS	0.285	–0.448–0.538	0.678	0.264–0.801
LV FAC	0.583	0.252–0.838	0.724	0.471–0.796
RV FAC	0.426	–0.374–0.924	0.623	–0.261–0.873
LVED area	0.535	0.255–0.793	0.723	0.617–0.835
LVED length	0.850	0.679–0.925	0.638	0.254–0.864
LVES area	0.628	0.589–0.830	0.628	0.374–0.734
LVES length	0.748	0.528–0.836	0.792	–0.571–0.832
RVED area	0.835	0.376–0.956	0.713	0.523–0.862
RVED length	0.829	0.636–0.952	0.628	0.358–0.824
RVES area	0.850	0.623–0.912	0.879	0.523–0.961
RVES length	0.927	0.529–0.964	0.815	0.347–0.963
LVEDD segment 1	0.720	0.543–0.792	0.738	0.627–0.953
LVEDD segment 9	0.739	0.528–0.891	0.834	0.581–0.957
LVEDD segment 17	0.747	0.438–0.952	0.832	0.537–0.934
RVEDD segment 1	0.755	0.623–0.815	0.834	0.652–0.958
RVEDD segment 9	0.729	0.527–0.823	0.678	0.415–0.892
RVEDD segment 17	0.730	0.468–0.924	0.734	0.316–0.859
LVSI segment 1	0.829	0.268–0.892	0.892	0.518–0.956
LVSI segment 9	0.793	0.682–0.892	0.842	0.437–0.975
LVSI segment 17	0.748	0.511–0.837	0.724	–0.261–0.834
RVSI segment 1	0.747	0.623–0.813	0.846	0.473–0.964
RVSI segment 9	0.713	0.521–0.958	0.823	0.467–0.926
RVSI segment 17	0.628	–0.173–0.752	0.813	0.624–0.962
LVFS segment 1	0.635	0.521–0.784	0.724	–0.472–0.834
LVFS segment 9	0.725	0.422–0.894	0.623	–0.164–0.827
LVFS segment 17	0.712	0.642–0.953	0.723	0.583–0.943
RVFS segment 1	0.528	–0.216–0.682	0.522	–1.496–0.634
RVFS segment 9	0.623	0.512–0.843	0.689	0.316–0.843
RVFS segment 17	0.538	0.282–0.732	0.752	0.271–0.831

ED, end-diastolic; ES, end-systolic; EDD, end-diastolic diameter; FS, fractional shortening; FAC, fractional area change; Fetal HQ, fetal heart quantification; GLS, global longitudinal strain; ICC, intraclass correlation coefficient; LV, left ventricle; RV, right ventricle; SI, sphericity index.

perspectives (25).

Studies have demonstrated that Fetal HQ technology significantly improves the detection of fetal ventricular deformation and rotation, thereby aiding in the early identification and diagnosis of fetal cardiac abnormalities. Furthermore, Fetal HQ technology enhances the precision of cardiac morphological analysis. Traditional 2D-STE exhibits limitations in structural analysis, particularly regarding complex myocardial fiber movements and ventricular rotation in fetal hearts. Fetal HQ technology employs multisegment analysis and advanced algorithms to measure GSI, segmental sphericity indices, and various ventricular dimensions. Research indicates that compared to traditional assessment methods, Fetal HQ technology provides more accurate assessments of fetal ventricular morphological changes, which are crucial for predicting perinatal outcomes and developing clinical intervention strategies (26). Additionally, Fetal HQ technology offers superior measurement repeatability and reliability. Traditional 2D-STE suffers from lower repeatability due to manual operation and variability in measurement angles. In contrast, Fetal HQ enhances measurement consistency through automated and standardized methods. Studies have revealed that Fetal HQ technology demonstrates markedly better repeatability in cardiac function assessment as compared to traditional 2D-STE (12). Given these advantages, our study employed Fetal HQ technology to assess fetal cardiac structure and function in cases of HDP, with the aim of clarifying how fetal cardiac function is affected by HDP and to compare it with the function in fetuses from normal pregnancies. This approach provides valuable scientific evidence and can enhance clinical diagnosis and intervention.

Our study's findings indicate that within the HDP group, the ED and ES areas and lengths of the LV were significantly larger than were those of the control group, although the volumes were smaller. Specifically, LV morphological indicators including LVED area, LVED length, and LVES area were higher while LVEDV was lower relative to the corresponding measures in the control group. This pattern suggests that increased afterload from hypertensive disorders causes the LV to enlarge in area and length but limits its volumetric expansion. Shen *et al.* employed Fetal HQ technology in a study of anemic pregnant women and found that maternal anemia did not significantly impact fetal heart size or systolic function but did alter cardiac morphology, leading to a more spherical heart and abnormal segments in the apical region of the left

ventricle (27).

Interestingly, in our study, in contrast to the control group, the HDP group exhibited markedly lower values in the RV, including for RVED area, RVED length, and RVES length. This implies that HDP may differentially affect the right side of the heart, potentially due to variations in ventricular loading conditions and the idiosyncrasies of the fetal circulatory system. Yovera *et al.* observed that gestational diabetes mellitus (GDM) was associated with decreased fetal RV function, which did not intensify with advancing GA (28).

The significantly higher LV global strain observed in the HDP group indicated altered cardiac function, particularly affecting the LV's longitudinal function. Only LV global strain demonstrated a statistical significance difference in the comparison of the HDP group and the control group ($P=0.006$), while other indicators did not. This suggests that LV global strain is more sensitive to changes in fetal cardiac function due to hypertension. Strain measures myocardial deformation, detecting subtle early changes in cardiac function. Conversely, other indicators such as ejection fraction and FAC may only reveal significant differences in more pronounced cardiac dysfunction. Additionally, HDP appears to impact the LV more than the RV, as the LV is more susceptible to hemodynamic changes. Chen *et al.* reported that fetuses of women with well-controlled GDM exhibited ventricular systolic abnormalities more commonly in the right ventricle, with transverse systolic abnormalities being more prevalent than global or longitudinal ones (29). The discrepancy between our findings and those of Chen *et al.* may arise from differences in how HDP and GDM affect fetal cardiac function. While HDP primarily affects LV function through altered hemodynamic status, GDM more commonly impacts RV function through direct myocardial damage caused by elevated blood glucose levels.

Our study also compared the ED values of the 24-segment model between the HDP and control groups. We observed significant increases in ED values in LV segments 12–22 and 24, as well as in the RV segments 12–17, 19, and 24. These findings indicate that different segments of the ventricles may undergo varying degrees of pressure load and adaptive responses under hypertensive conditions, resulting in significant changes in ED values.

Additionally, in the HDP group, segmental SI values in both the LV (segments 8–24) and RV (segments 16–24) were notably lower. The decrease in SI values may reflect underlying pathophysiological changes in cardiac function due to HDP. In the LV, decreased SI values could indicate

diminished myocardial contractility or altered perfusion resulting from increased afterload and reduced myocardial oxygen delivery. Similarly, decreased SI values in the RV may suggest impaired function or increased strain, possibly due to elevated pressures or volume overload. These findings underscore the need for a comprehensive cardiac assessment in cases of HDP, as impaired ventricular function could lead to adverse outcomes for both the mother and fetus, including compromised fetal growth and elevated likelihood of maternal cardiovascular disorders.

The comparison of the 24-segment ventricular FS values and FS Z scores underscore the significant impacts of maternal hypertension on fetal cardiac function in cases of HDP. As compared to the control group, the HDP group had lower FS values in the LV and RV across multiple segments, particularly in LV segments 3–24 and RV segments 4–23, with significant differences in segments 12 and 19 ($P < 0.001$). These findings align with other studies suggesting that maternal hypertension disrupts fetal hemodynamics and placental perfusion, compromising cardiac function (12,30). The FS Z scores, which standardize ventricular function relative to normative data, further point to the global impairment in the HDP group. Segments including LV 12 and 16 and RV 12 and 19 showed significantly lower Z scores ($P < 0.05$), emphasizing the broader impact of HDP on fetal cardiac development.

The minor disparities between FS values and Z scores suggest different dimensions of cardiac dysfunction. FS values directly measure ventricular contractile function, while Z scores assess relative impairment against expected norms, revealing more pronounced deficits in cases of HDP, as shown in the study by Youssef *et al.* (31). This suggests that fetuses exposed to hypertensive conditions face not only functional impairments but also an inability to adapt to physiological demands, exacerbating the severity of dysfunction. Factors such as altered placental blood flow, fetal hypoxia, and cardiac remodeling may contribute to this condition. Compensatory mechanisms and pathophysiological processes such as myocardial ischemia or reduced myocardial compliance further underline the complex interplay between maternal hypertension and fetal cardiac dysfunction.

Finally, the findings strongly support the reliability of Fetal HQ, confirming its utility in clinical settings for the consistent and reproducible assessment of fetal cardiac function. Additionally, the high intra-observer and interobserver reliability observed in our study reinforces its potential for use in clinical practice. The robust reliability of

these measurements is crucial for accurately diagnosing and managing fetal cardiac abnormalities, ensuring healthcare professionals can depend on these parameters for precise evaluations.

Conclusions

This study applied Fetal HQ technology to investigate the alterations in the fetal heart within pregnancies affected by HDP. The results indicated that there were significant alterations in the heart structure and function in the HDP group, including larger LVs and increased strain. Fetal HQ effectively detected these abnormalities, underscoring its value in the early diagnosis and management of fetal heart issues in HDP pregnancies.

Acknowledgments

None.

Footnote

Reporting Checklist: The authors have completed the STROBE reporting checklist. Available at <https://qims.amegroups.com/article/view/10.21037/qims-24-1553/rc>

Funding: This work was supported by the Key R&D Foundation of Hubei Province (grant No. 2022BCE004), the National College Student Innovation and Entrepreneurship Training Program of Hubei University of Medicine (grant No. 202210929019), and the Science and Technology foundation of Xiangyang (grant No. 2022YL26A).

Conflicts of Interest: All authors have completed the ICMJE uniform disclosure form (available at <https://qims.amegroups.com/article/view/10.21037/qims-24-1553/coif>). The authors have no conflicts of interest to declare.

Ethical Statement: The authors are accountable for all aspects of the work in ensuring that questions related to the accuracy or integrity of any part of the work are appropriately investigated and resolved. This study was conducted in accordance with the Declaration of Helsinki (as revised in 2013) and was approved by the Ethics Committee of the Xiangyang No. 1 People's Hospital, School of Medicine, Wuhan University of Science and Technology (approval No. 2021KYLX02). Informed consent was

obtained from all participants.

Open Access Statement: This is an Open Access article distributed in accordance with the Creative Commons Attribution-NonCommercial-NoDerivs 4.0 International License (CC BY-NC-ND 4.0), which permits the non-commercial replication and distribution of the article with the strict proviso that no changes or edits are made and the original work is properly cited (including links to both the formal publication through the relevant DOI and the license). See: <https://creativecommons.org/licenses/by-nc-nd/4.0/>.

References

1. Agrawal A, Wenger NK. Hypertension During Pregnancy. *Curr Hypertens Rep* 2020;22:64.
2. Keskinliç B, Engin-Üstün Y, Sanisoğlu S, Şahin Uygun D, Keskin HL, Karaahmetoğlu S, Özcan A, Esen M, Alkan A, Kabasakal A, Şencan İ. Maternal mortality due to hypertensive disorders in pregnancy, childbirth, and the puerperium between 2012 and 2015 in Turkey: A nation-based study. *J Turk Ger Gynecol Assoc* 2017;18:20-5.
3. Sinkey RG, Battarbee AN, Bello NA, Ives CW, Oparil S, Tita ATN. Prevention, Diagnosis, and Management of Hypertensive Disorders of Pregnancy: a Comparison of International Guidelines. *Curr Hypertens Rep* 2020;22:66.
4. Brown MA, Magee LA, Kenny LC, Karumanchi SA, McCarthy FP, Saito S, Hall DR, Warren CE, Adoyi G, Ishaku S; International Society for the Study of Hypertension in Pregnancy (ISSHP). Hypertensive Disorders of Pregnancy: ISSHP Classification, Diagnosis, and Management Recommendations for International Practice. *Hypertension* 2018;72:24-43.
5. Thornburg KL, Drake R, Valent AM. Maternal Hypertension Affects Heart Growth in Offspring. *J Am Heart Assoc* 2020;9:e016538.
6. Zhou H, Zou X, Hu B. Focused Cardiac Ultrasonography for Left Ventricular Systolic Function. *N Engl J Med* 2020;382:977.
7. Salmasi AM, Salmasi S, Nicolaides AN. Doppler ultrasound in assessing systolic left ventricular function in cardiovascular patients. *Int Angiol* 1990;9:29-37.
8. Thomas JD, Popović ZB. Assessment of left ventricular function by cardiac ultrasound. *J Am Coll Cardiol* 2006;48:2012-25.
9. Axt-Fliedner R, Graupner O, Kaweckı A, Degenhardt J, Herrmann J, Tenzer A, Doelle A, Willruth A, Steinhart J, Gembruch U, Bahlmann F, Enzensberger C; Fetal Cardiac Imaging Research Group, Germany. Evaluation of right ventricular function in fetuses with hypoplastic left heart syndrome using tissue Doppler techniques. *Ultrasound Obstet Gynecol* 2015;45:670-7.
10. DeVore GR. Assessing fetal cardiac ventricular function. *Semin Fetal Neonatal Med* 2005;10:515-41.
11. Zhang W, Zhang B, Wu T, Li Y, Qi X, Tian Y, Chen J, Luo H. Value of two-dimensional speckle-tracking echocardiography in evaluation of cardiac function in small fetuses. *Quant Imaging Med Surg* 2024;14:8155-66.
12. Nogué L, Gómez O, Izquierdo N, Mula C, Masoller N, Martínez JM, Gratacós E, Devore G, Crispi F, Bennasar M. Feasibility of 4D-Spatio Temporal Image Correlation (STIC) in the Comprehensive Assessment of the Fetal Heart Using FetalHQ®. *J Clin Med* 2022;11:1414.
13. Chappell LC, Tucker KL, Galal U, Yu LM, Campbell H, Rivero-Arias O, et al. Effect of Self-monitoring of Blood Pressure on Blood Pressure Control in Pregnant Individuals With Chronic or Gestational Hypertension: The BUMP 2 Randomized Clinical Trial. *JAMA* 2022;327:1666-78.
14. Magro-Malosso ER, Saccone G, Di Tommaso M, Roman A, Berghella V. Exercise during pregnancy and risk of gestational hypertensive disorders: a systematic review and meta-analysis. *Acta Obstet Gynecol Scand* 2017;96:921-31.
15. Cífková R. Hypertension in Pregnancy: A Diagnostic and Therapeutic Overview. *High Blood Press Cardiovasc Prev* 2023;30:289-303.
16. Podymow T, August P. New Evidence in the Management of Chronic Hypertension in Pregnancy. *Semin Nephrol* 2017;37:398-403.
17. Ramlakhan KP, Johnson MR, Roos-Hesselink JW. Pregnancy and cardiovascular disease. *Nat Rev Cardiol* 2020;17:718-31.
18. Maraboto Gonzalez CA, Dudzinski DM. Back to basics: M-mode and left ventricular function. *J Clin Ultrasound* 2022;50:601-3.
19. Schober KE, Chetboul V. Echocardiographic evaluation of left ventricular diastolic function in cats: Hemodynamic determinants and pattern recognition. *J Vet Cardiol* 2015;17 Suppl 1:S102-33.
20. Zhao L, Wu P, Jiao X, Zhang M, Jing W, Wu Y, Chen S. Characteristics and outcomes of fetal ventricular aneurysm and diverticulum: combining the use of a new technique, fetal HQ. *Front Pediatr* 2023;11:1165972.
21. van Oostrum NHM, Derks K, van der Woude DAA, Clur SA, Oei SG, van Laar JOEH. Two-dimensional Speckle

- tracking echocardiography in Fetal Growth Restriction: a systematic review. *Eur J Obstet Gynecol Reprod Biol* 2020;254:87-94.
22. van Oostrum NHM, de Vet CM, Clur SB, van der Woude DAA, van den Heuvel ER, Oei SG, van Laar JOEH. Fetal myocardial deformation measured with two-dimensional speckle-tracking echocardiography: longitudinal prospective cohort study of 124 healthy fetuses. *Ultrasound Obstet Gynecol* 2022;59:651-9.
 23. Song Y, Yin H, Wang W, Zou YF, Liu DQ, Zhang G, Ji XP. Evaluation of fetal cardiac functions in the setting of maternal diabetes: Application of the global spherical index, global strain and fractional area change by the speckle tracking technique. *Eur J Obstet Gynecol Reprod Biol* 2021;264:162-7.
 24. Domínguez-Gallardo C, Ginjaume-García N, Ullmo J, Fernández-Oliva A, Parra J, Vázquez A, Cruz-Lemini M, Llurba E. Longitudinal Behavior of Left-Ventricular Strain in Fetal Growth Restriction. *Diagnostics (Basel)* 2023.
 25. Wang W, Liu JF, Yin H, Wang L, Zhang G, Song LL, Song Y. Evaluation of fetal cardiac function in fetal growth restriction via fetal HQ analysis based on two-dimensional STI. *J Obstet Gynaecol Res* 2023;49:1514-24.
 26. Vaidyanathan B, Soman S, Karmegaraj B. Utility of the novel fetal heart quantification (fetal HQ) technique in diagnosing ventricular interdependence and biventricular dysfunction in a case of prenatally diagnosed Uhl's anomaly. *Echocardiography* 2024;4:e15862.
 27. Shen Y, Tan F, Yang J, Fan S, Zhang L, Ji X. A preliminary study on fetal cardiac morphology and systolic function of normal and anemic pregnant women by fetal heart quantification technology. *Transl Pediatr* 2022;11:1336-45.
 28. Yovera L, Zaharia M, Jachymski T, Velicu-Scraba O, Coronel C, de Paco Matallana C, Georgiopoulos G, Nicolaides KH, Charakida M. Impact of gestational diabetes mellitus on fetal cardiac morphology and function: cohort comparison of second- and third-trimester fetuses. *Ultrasound Obstet Gynecol* 2021;57:607-13.
 29. Chen Y, Chen Q, Wu Y, Wang H, Fan Q, Lei W, Zhang R, Liang Y, Wang H. Fetal cardiac geometry and function in pregnancies with well-controlled gestational diabetes mellitus using Fetal HQ. *J Matern Fetal Neonatal Med* 2022;35:8331-7.
 30. McClements L, Richards C, Patel N, Chen H, Sesperez K, Bubb KJ, Karlstaedt A, Aksentijevic D. Impact of reduced uterine perfusion pressure model of preeclampsia on metabolism of placenta, maternal and fetal hearts. *Sci Rep* 2022;12:1111.
 31. Youssef L, Miranda J, Paules C, Garcia-Otero L, Vellvé K, Kalapotharakos G, Sepulveda-Martinez A, Crovetto F, Gomez O, Gratacós E, Crispi F. Fetal cardiac remodeling and dysfunction is associated with both preeclampsia and fetal growth restriction. *Am J Obstet Gynecol* 2020;222:79.e1-9.

Cite this article as: Peng Y, Feng W, Yu CX, Chang CH, Liao X, Gan L, Zhang JQ. Fetal heart quantification ultrasound technology for the quantitative analysis of fetal cardiac morphology and function in hypertensive disorders of pregnancy. *Quant Imaging Med Surg* 2025;15(4):3517-3531. doi: 10.21037/qims-24-1553